Journal of Applied Electrochemistry **31**: 1131–1140, 2001.

The role of chloride ions and pH in the corrosion and pitting of Al–Si alloys

A.A. MAZHAR[1], S.T. ARAB[2] and E.A. NOOR[2]
[1]*Chemistry Department, Faculty of Science, Cairo University, Giza, Egypt*
[2]*Chemistry Department, Girls' College of Education, PO Box 9470 Jeddah 21413, Kingdom of Saudi Arabia*

Received 11 October 1999; accepted in revised form 31 May 2000

Key words: Al–Si alloys, chloride ions, corrosion, pH, pitting

Abstract

The role of chloride ions in the pitting corrosion of some Al–Si alloys was investigated by chemical, polarization and EIS measurements, as well as SEM studies. Differences in corrosion rates of pure aluminium and the alloys are discussed. The capacitive behaviour of the oxide covered surface is replaced by resistive behaviour as immersion time increases in HCl solutions. At neutral pH corrosion currents increase then decrease with chloride ion concentrations. Pitting by chloride ions initiates more readily in acidic media.

1. Introduction

Aluminium finds extensive applications in the automotive industry as a result of emphasis on weight reduction to allow decreases in fuel costs. Thin and reproducible oxide layers form on aluminium after mechanical polishing and are stable under atmospheric conditions but thicken rapidly in solution so that the oxide reaches about 1000 times thicker (about 5000 nm) than the layer formed in air [1]. Corrosion of aluminium is thought to occur by ionic migration followed by dissolution at the oxide/electrolyte interface [2]. Due to its relative mechanical weakness it is usually strengthened by alloying, which may cause reduced corrosion resistance. The Al–Si alloys are among the most important commercial alloys. Al–Si is a simple eutectic system with two solid solution phases, the eutectic composition is 12.2 ± 0.1 at % Si [3]. Silicon exhibits low solubility in aluminium, < 0.1 wt % at 150 °C [3]. The presence of many alloying additives with limited solubilities in aluminium has been shown to promote localized corrosion [4].

Although aluminium passivates in H_2SO_4 due to formation of a porous oxide film [5], HCl gives rise to rapid aluminium corrosion [6]. The presence of chloride ions in aqueous media in contact with aluminium metal [7] or aluminium alloys [8], causes pitting attack. The presence of chloride ions was found to accelerate the corrosion of aluminium in aqueous media; the corrosion depended strongly on the pH of the solution [6]. Also, in acidic and alkaline media, where the solubility of aluminium oxide is enhanced, aluminium corrodes more rapidly [9]. Thus, the passivation of aluminium can be suppressed by lowering or increasing the pH, as well as by addition of chloride ions [6, 10]. In this study, the role of chloride ions and pH on the passivation and corrosion of some Al–Si alloys is investigated.

2. Experimental details

Analyses of the three Al–Si alloys and commercially pure aluminium are given in Table 1. According to the Al–Si phase diagram [3] alloy I is a hypoeutectic alloy (Al + eutectic), alloy II is almost formed of the eutectic, while III is a hypereutectic alloy (Si + eutectic).

Samples used in chemical measurements were 5 cm long and 1 cm in diameter. Electrodes used in potentiostatic polarization and electron impedance spectroscopy, (EIS), were in the form of rods embedded in glass tubes just larger than the sample and fixed with Araldite adhesive (Ciba Geigy, Switzerland) so that when immersed in the test solution the area exposed was 0.785 and 0.204 cm^2 in polarization and EIS measurements, respectively. The electrodes were previously polished mechanically with finer grade of emery paper up to 4/0, washed with deionized water and rinsed with the test solution. The samples used in chemical measurements were mechanically polished and washed with deionized water decreased with acetone and dried with air, and immersed immediately in the test solution. All reagents were A.R. grade (BDH) except HCl (Fluka) and boric acid (Merck).

Experiments were carried out at a constant temperature of 30 ± 0.2 °C, adjusted by using an ultrathermostat (Julabo μ 3, no. 8311). Solutions were unstirred and, in polarization experiments were dearated by ultra pure nitrogen (99.999% purity). The reference electrode was Ag/AgCl, and the auxillary electrode a Pt wire in polarization measurements or a Pt sheet (about 4 cm^2) in EIS.

Table 1. Composition of Al–Si alloys and pure Al (by weight percent)

	Si	Cu	Zn	Pb	Co	Ni	Fe	Cr	Al
Alloy I	7.0	0.048	0.004	0.001	< 0.02	0.023	0.136	0.006	Balance
Alloy II	11.0	0.123	0.014	0.002	< 0.05	0.073	0.113	0.025	
Alloy III	22.0	0.282	0.021	0.007	< 0.05	0.385	0.179	0.056	
Pure Al	–	0.002	0.003	0.100	< 0.05	0.011	0.179	0.082	

Potentiostatic polarization was carried out using an AMEL potentiostat, (model 533, Italy) with positive feedback for *iR* drop compensation. EIS measurements were carried out by employing an impedance spectrum analyser (Thales IM 6, Germany) connected to a Samsung computer (Sync Master 15 GLi). All experiments were in the frequency range 100 kHz to 0.1 Hz. The input signal amplitude was 10 mV peak to peak in both the high and low frequency ranges. Scanning electron microscopy, (SEM), of the electrode surface was carried out using a Jeol/JSM T20 (Japan) scanning electron microscope. The alloys were etched in a solution formed of conc. HF (10 ml) + conc. HCl (15 ml) + 90 ml H_2O, while pure Al was etched in 15% NaOH. SEM for the alloys and for pure Al was also conducted after immersion of the polished samples for 90 min in 0.5 M HCl. Energy diffraction X-ray analysis (EDX) was carried on the samples before and after immersion in 0.5 M HCl. The EDX unit was attached to Jeol/JSM-5400 (Japan) scanning electron microscope.

The pH of the sulphate solution was adjusted at pH 2, 7 or 10 by addition of carbonate free NaOH. The Jenway pH meter (model 3015) was calibrated before and after each measurement with National Institute of Standards and Technology (NIST) solutions (pH 4.01 and 6.865).

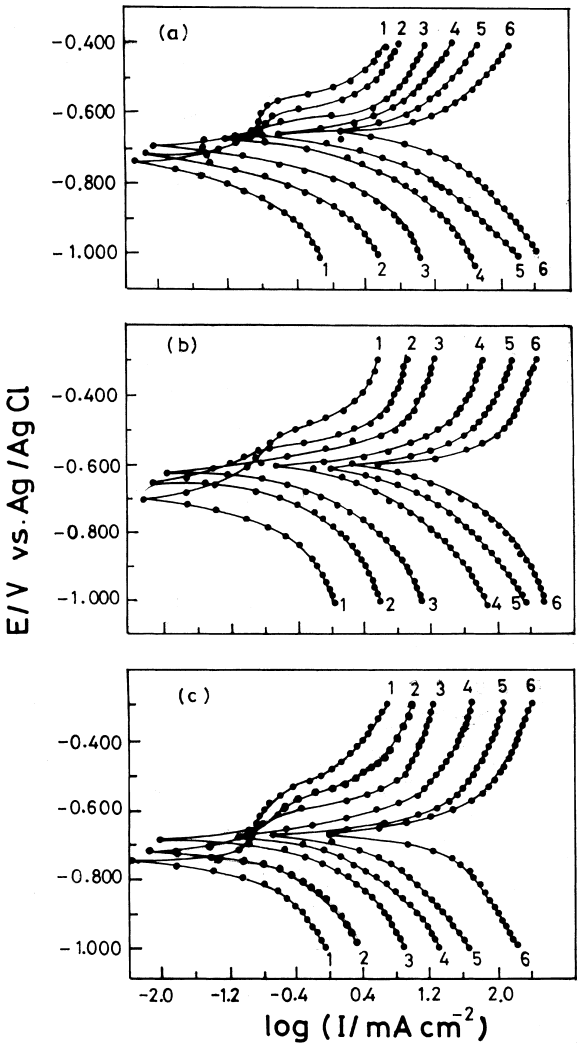

Fig. 1. Polarization curves for alloy (a) I, (b) II and (c) III as a function of HCl concentration: (1) 0.10, (2) 0.025, (3) 0.05, (4) 0.15, (5) 0.25 and (6) 0.50 M.

3. Results and discussion

3.1. *Effect of HCl concentration*

The results of polarization measurements for the three alloys in HCl solutions are shown in Figure 1. At the lowest Cl^- concentration, a more or less passive behaviour is detected for alloy I (Figure 1(a)) around a current density of 0.14 mA cm^{-2}, followed by a sharp current increase at −0.57 V, which indicates onset of localized attack, or pitting. The passive region may be attributed to existence of the air formed oxide film [11]. The oxide film cannot be ignored, even in highly acidic media, such as HCl [12].

At the potential at which pitting starts, E_{pit}, the potential current relationship tends to assume a zero slope. In the potential region bounded by E_{pit} and the onset potential for hydrogen evolution the aluminium corrosion resistance has been reported to be greatest [13].

The corrosion potential, E_{corr}, was obtained by the Tafel extrapolation. E_{corr} shifts to less negative potentials with increase in HCl concentration. This is due to the decrease in pH. The aluminium surfaces are positively charged in acid media, since the pH of the potential of zero charge (p.z.c.) for aluminium at the oxide/solution interphase in 9.0–9.1 [14]. Thus, as the pH decreases, the alloy surface acquires a less negative potential.

With increasing acid concentration the cathodic branch showed a marked increase in c.d. for the three alloys, while E_{pit} was found to shift to more negative values. This caused a decrease in the passive range bounded by E_{pit} and E_{corr}, which is attributed to a greater number of defects in the oxide layer. The spectra obtained in an EIS study on the corrosion behaviour of aluminium indicated that the electrochemical processes in the passive region are controlled mainly by multistep dissolution, ionic migration through the oxide layer and the influence of chloride ions [15]. This passive region was previously attributed to the existence of an oxide film on the metal surface [11]. At E_{pit} the passive oxide film is replaced by an unstable salt film which undergoes dissolution easily above E_{pit} [16]. At high anodic

polarization, Vetter suggested the occurrence of a salt layer within the pits [17].

The shift of E_{pit} to more negative values indicates ease of the corrosion process or decrease in alloy resistance due to active dissolution (localized attack). Values of E_{pit} in 10^{-2} M HCl are −0.565, −0.535 and −0.575 V for alloys I, II and III, respectively, while values estimated for the passive potential, E_{pass}, in the same order are −0.675, −0.605 and −0.695 V. The passive region is the least for alloy II and greatest for alloy III, indicating that the former is the least protected while the latter is the most protected of the alloys.

Pitting corrosion is an anodic electrochemical process which depends on the surface excess of chloride ions, which, in turn, is determined by the bulk chloride ion concentration through transport, adsorption and/or chemical reactions [18]. At low concentrations the passive oxide film locally ruptures and heals spontaneously, as proved by a.c. impedance measurements [19]. Higher concentrations prevent the healing process. This causes a decrease in the passive region. At progressively higher concentrations the passive regions are completely absent which indicates direct attack of the alloys even at low anodic polarizations. This supports the notion that chloride ions are responsible for attack of the film and subsequent dissolution of the oxide layer. The attack by chloride ions occurs by formation of complexes containing chloride ions at the film/solution interface which are more soluble than complexes formed in absence of chloride ions according to [10] the following:

$$\mathrm{Al} + n\mathrm{Cl}^- \rightarrow \mathrm{AlCl}_n^{(n-3)-} + 3\mathrm{e}^- \qquad (1)$$

which causes thinning of the passive layer and pitting corrosion.

The corrosion current, i_{corr}, was obtained by the Tafel extrapolation. Values of i_{corr} increased with increase in acid concentration for any of the alloys, which according to the Stern–Geary relation [20], indicates decrease in the polarization resistance as the acid concentration increases. At one and the same concentration the value of i_{corr} followed the order II > I > III, which indicates that alloy II has the highest susceptibility to corrosion.

Figure 2 shows the dependence of E_{corr} and i_{corr} on acid concentration. The linear relations in case of E_{corr} can be represented by the equation [21]:

$$E_{corr} = E^{\circ}_{corr} + \frac{2.3\,RT}{nF}\log c \qquad (2)$$

where E°_{corr} is the corrosion potential when the concentration is equal to unity. The deviation of (n) from the expected value may be related to a multistep process of film formation.

The relation between i_{corr} and concentration follows the relations:

$$i_{corr} = a + b\log c \qquad (3)$$

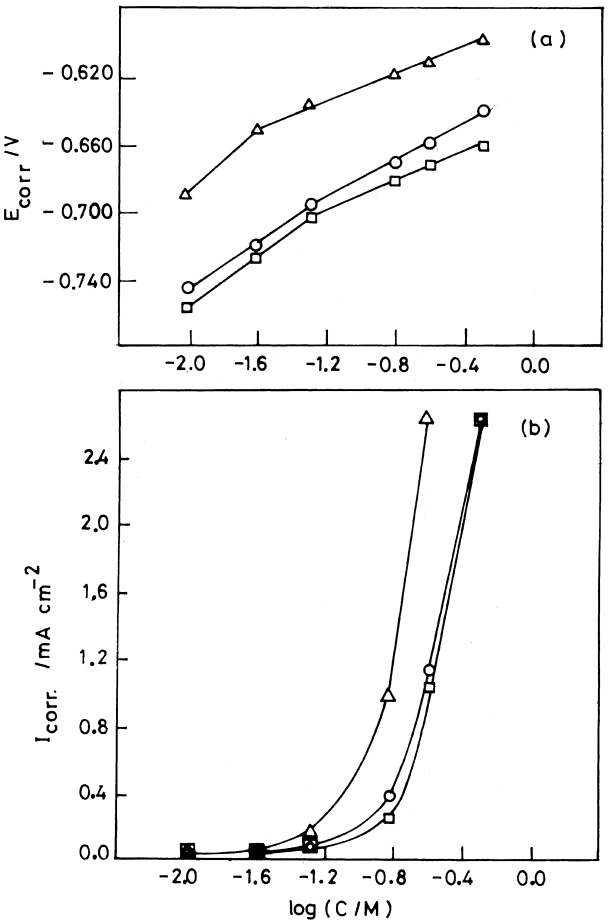

Fig. 2. Dependence of (a) E_{corr} and (b) i_{corr} on HCl concentration for alloy (○) I, (△) II and (□) III.

where a and b are characteristics dependent on the corroding surface. At low concentrations the dependence of i_{corr} on concentrations is limited, but shows a marked dependence at higher concentrations. This is attributed to a more open structure of the oxide with a higher number of defects under these conditions.

The polarization behaviour of the alloys was compared to pure Al in 0.5 M HCl. The value of i_{corr} was also found to be in the order II > I > III > Al, which indicates that pure Al is less susceptible to corrosion than any of the alloys, in agreement with previous observations [4].

These results were confirmed by chemical measurements. In the hydrogen evolution measurements (HEM) an induction period was observed at low acid concentrations for all alloys. During the induction period the acid reacts with the air formed oxide film. The induction period was observed to decrease with increase of acid concentration and therefore the activation process is dependent on the Cl^- concentration. During the induction period, Cl^- penetrate below the air formed oxide, thus leading to loss of protection by the native oxide. At the highest Cl^- concentrations the attack was instantaneous. At any concentration the induction period followed the same order of corrosion susceptibility of the alloys (i.e., II > I > III). The rate of hydrogen evolution, R (ml cm^{-2} min^{-1}) as well as the rate of mass

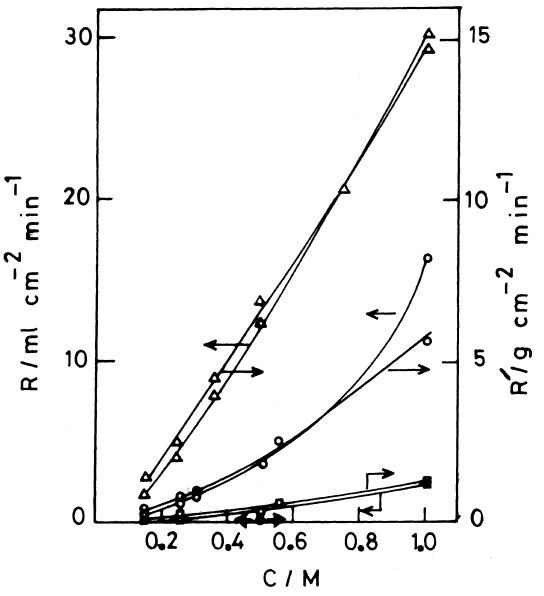

Fig. 3. Effect of HCl concentration on (——) R and (- - -) R', symbols as in Figure 2, (●) pure Al.

loss, R' (g cm^{-2} min^{-1}) are plotted as function of acid concentration for all alloys, Figure 3. The results of both HEM and mass loss measurements confirm the order of corrosion rates for the alloys and pure Al obtained by polarization measurements.

3.2. *EIS*

EIS measurements were conducted at open circuit conditions after a steady state potential was attained in aerated 0.5 M HCl for alloy II. Figure 4(a) shows the Nyquist plots after different time intervals from the beginning of immersion. The high frequency capacitive semicircles are related to the dielectric properties and thickness of the barrier film [22], while the incomplete inductive loop may indicate the presence of at least one adsorbed species [19] or the occurence of localized corrosion [22]. In the latter case high field ionic migration of Al^{3+} and O^{2-} will be involved, and possibly of Al^{+} generated at the metal/oxide interface to the oxide–electrolyte interface [2]. While the occurence of localized corrosion is certain in the present case, presence of an adsorbed species is also highly probable. The well defined capacitive semicircles suggest that the corrosion process occurs under activation control [23]. With increasing time intervals the polarization resistance, R_p, which can be estimated from the diameters of the capacitive semicircles, is found to decrease. This is caused by the attack of chloride ions, the extent of which increases with time. After 60 min immersion the inductive behaviour becomes progressively important, as can be judged from the relative increase of the diameter of the inductive loop as compared to the diameter of the capacitive loop.

The Bode plot, Figure 4(b), shows also significant changes with time. The maximum phase shift, θ_{max},

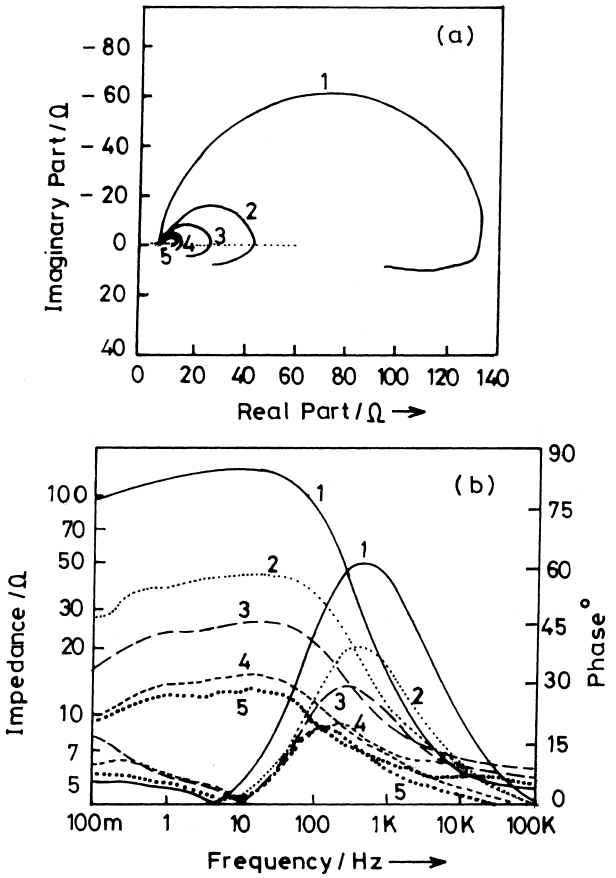

Fig. 4. Nyquist (a) and Bode (b) plots for alloy II in 0.5 M HCl after different time intervals of immersion (1) 5, (2) 30, (3) 60, (4) 90 and (5) 120 min.

decreases with time, shifting meanwhile to lower frequencies which suggests a slight increase in the area of the metal exposed to the electrolyte. The decrease in θ_{max} with time indicates departure from capacitive behaviour towards approximately resistive behaviour for the circuit. There is an inflection in θ–log f relation at low frequencies which is related to different time constants [24]. The inductive behaviour caused by the localized process is apparent as the impedance decreases at low frequencies [25]. The difference between the high frequency limit and low frequency limit in the Bode plot is equal to R_p, the polarization resistance of the dissolution and repassivation processes in addition to the electronic conductivity of the film. As R_p decreases with time (at $f = 0.16$ Hz where log ω = log $2\pi f$ = zero) the capacitance, C, increases. This is related to the decrease in the effective thickness of the oxide, as chloride ions which are chemically bonded to the surface [18] are subsequently removed in the form of aluminium chloro- and oxohydroxo-complexes. The decrease in both impedance (at $f = 0.16$ Hz) and θ_{max} indicates a decrease in polarization resistance with immersion time, as the oxide film is attacked and removed from the surface.

After 60 min immersion of the three alloys in 0.5 M HCl at open circuit conditions produced the Nyquist plot, Figure 5(a). It is clear that both capacitive and inductive loops are larger in case of alloy III than the

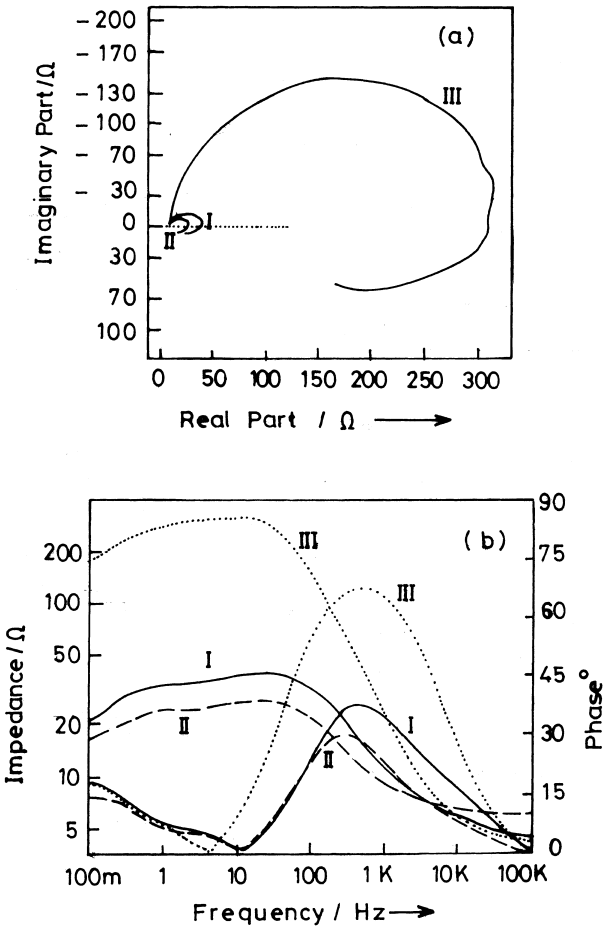

Fig. 5. Nyquist (a) and Bode (b) plots for the three alloys after 60 min immersion in 0.5 M HCl.

other two alloys. The polarization resistance as determined from the capacitive loop is in the order II < I < III, which indicates that alloy III has the best electrochemical properties. This is also associated with the larger low–frequency inductive part of the impedance which is mainly determined by the faradaic processes of the system studied.

The Bode plot for the alloys is shown in Figure 5(b). The deviation of the log Z–log f relation at intermediate frequencies from the value of −1, and the depression of the capacitive semicircles below the axis (Figure 5(a)) are often referred to as frequency dispersions, and are attributed to inhomogenities in the solid surface [22]. The inductive behaviour due to the localized process is also clear for all alloys, as the impedance decreases at low frequencies. The second time constant is apparent for all alloys as can be judged from the inflection in the θ–log f relation. This second time constant may indicate the presence of a salt film [26]. The polarization resistance for the alloys, as estimated from the difference in the high and low frequency limits of the impedance in the Bode plot are in the order II < I < III. This is the same order of θ_{max} values, in accord with the decrease of capacitive properties of the oxide covered electrode. The foregoing results support the conclusion that the order of corrosion susceptibility of the alloys is II > I > III.

3.3. *SEM*

Micrographs for pure Al and the alloys are shown in Figure 6. These studies indicate that alloy II is almost completely formed of the eutectic. Very fine Al grains can be seen together with the eutectic, as expected [3]. Alloy I contains large Al grains surrounded by the eutectic, while alloy III is composed of primary Si and the eutectic.

After 90 min immersion of the samples in 0.5 N HCl SEM produced are shown in Figure 7 [7]. While pure Al is attacked only by general corrosion, the alloys are attacked also by pitting corrosion. There are significant differences in the pitting observed. The pits in alloy I and III are distinct and spherical, indicating improved film quality [27]. The pits in alloy I were numerous and small, while the few pits that could be detected on the surface of alloy III are large. Severe pitting is observed in case of alloy II, the pits are deep and irregular.

The lower polarization resistance of the alloys as compared to pure Al is attributed to the localized galvanic couples present in the alloy [28]. Among the three alloys, the lowest polarization resistance was observed for alloy II. The incorporation of elemental Al in the eutectic in alloy I, or elemental Si in case of alloy III causes stabilization of the oxide film [29]. EDX studies revealed that the surface concentration of Al or Si is not affected by treatment with HCl in case of alloy II, which indicates homogenous corrosion of the alloy. The high corrosion rate of alloy II, which is mainly formed of the eutectic, is attributed to the high stress in the eutectic net. In case of alloy I, EDX studies showed a decrease in the surface concentration of Al by 4.5%, due to the severe attack of Al grains by HCl. Alloy III showed an increase in the surface Si content by 3.5% which is attributed to the fact that primary Si is not attacked by HCl, and corrosion occurs mainly by attack of the eutectic net. The present results agree with the observation of the decrease in the corrosion rate of an Al–Si alloy when the matrix contained more than 12% Si by mass [30].

3.4. *Effect of Cl^- concentration at constant pH*

It is well known that both pH and chloride ion concentration play important roles in the corrosion of Al and its alloys. In this part, a study was made on the effect of Cl^- concentration on the electrochemical properties of alloy II at constant pH values. The results are shown in Figure 8, with the pH of the solutions adjusted at values of 2.0, 7.0 and 10.0, respectively. Sulphate medium was chosen as background electrolyte which neither causes nor inhibits efficiently the pitting corrosion of aluminium, and is often selected as background electrolyte for E_{pit} determinations [1, 18]. The passivity of aluminium in sulphate solutions is known to be due to formation of a porous oxide film on the surface [5]. Suppression of the passivity by addition of the aggressive chloride ions was attempted at pH values 2.0, 7.0 and 10.0 to clarify the degree of attack at these pH values.

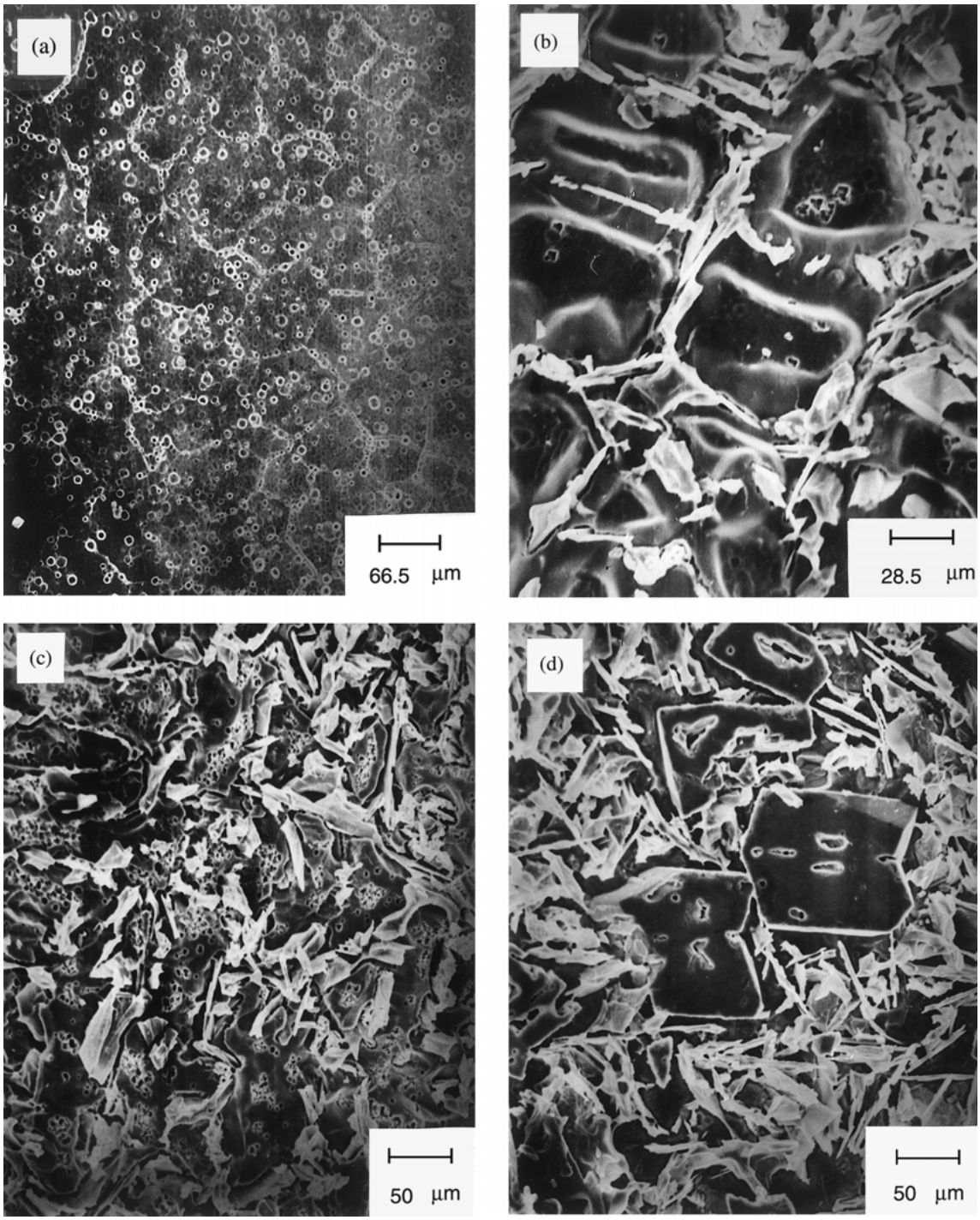

Fig. 6. SEM for etched (a) pure Al:Al grains attacked by the etchent (b) alloy I:Al grains surrounded by the acicular eutectic (c) alloy II:microstructure formed mainly of the eutectic with fine Al grains (d) alloy III:primary Si (H-shaped) surrounded by acicular eutectic.

The main feature in the figures is that the passivity range is suppressed with increase of Cl^- concentration, irrespective of the pH value of the solution. Increasing the halide concentration moves the p.z.c. to the active direction [31]. The difference in the magnitude of the change in potential with increase in Cl^- concentration at pH 2.0 or 10.0, compared to that at pH 7.0, is related to the nature and stability of the film present on the metal surface at the studied pH values [29].

At pH 2 and 10, the relation between E_{corr} and Cl^- concentration followed the equation:

$$E_{corr} = E^{\circ}_{corr} - \frac{2.3\,RT}{nF}\log[Cl^-] \tag{4}$$

where E°_{corr} is the value of E_{corr} at Cl^- concentration equal to unity. The latter relation was reported recently for the corrosion of Mg–Al alloy in alkaline solutions (pH 10.5) [32]. Calculated values for (n) varied between

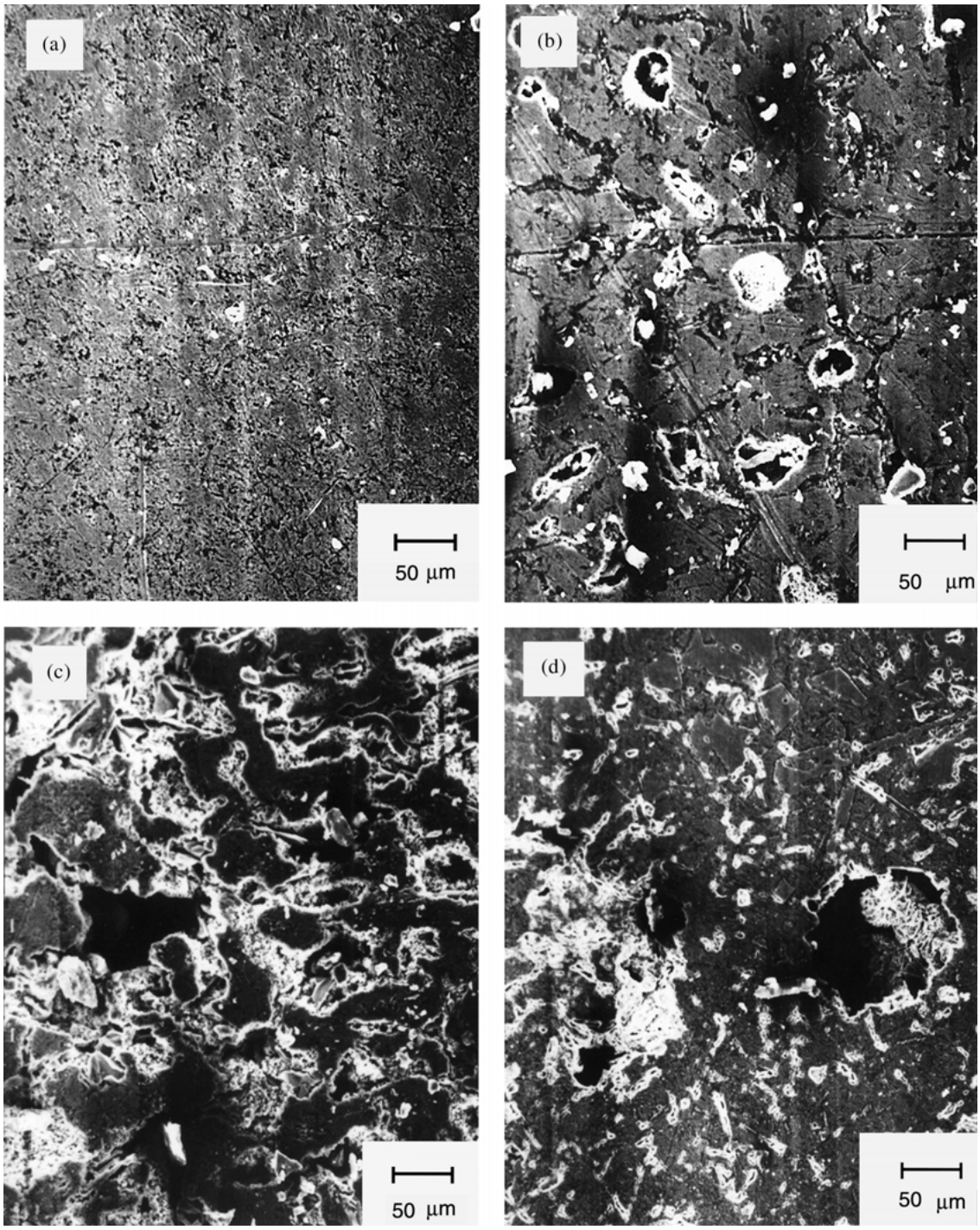

Fig. 7. SEM after 90 min immersion in 0.5 M HCl (a) pure Al: general corrosion (b) alloy I: general and pitting corrosion, pits are distinct and spherical (c) alloy II: severe pitting, pits are deep and irregular (d) alloy III: general and pitting corrosion, pits are few over the entire surface (spherical).

2 at pH 10 to 3 at pH 2, which suggests that the corrosion process consists of a number of steps, one of which permits formation of compounds containing Cl^- ions [33].

Values of i_{corr} at pH 2.0 were found to increase with increase in Cl^- concentration, due to increase in both cathodic and anodic currents, that is, cathodic and anodic reaction rates. At pH 7.0, corresponding to conditions of best oxide stability, values of i_{corr} increase at first with increase in Cl^- concentration then decrease for concentrations above 0.1 N Cl^-, due to the synergistic effect of Cl^- and SO_4^{2-} [34]. Similar results were obtained for Al–Cu alloy at pH 6.0, which exhibits an initial increase in corrosion with Cl^- concentration up to 3.5% NaCl, followed by a gradual decrease [10]. It was explained that at neutral pH values, where OH^- concentration is relatively low ($\sim 10^{-7}$ mol l^{-1}), low Cl^- concentration can accelerate corrosion by attacking

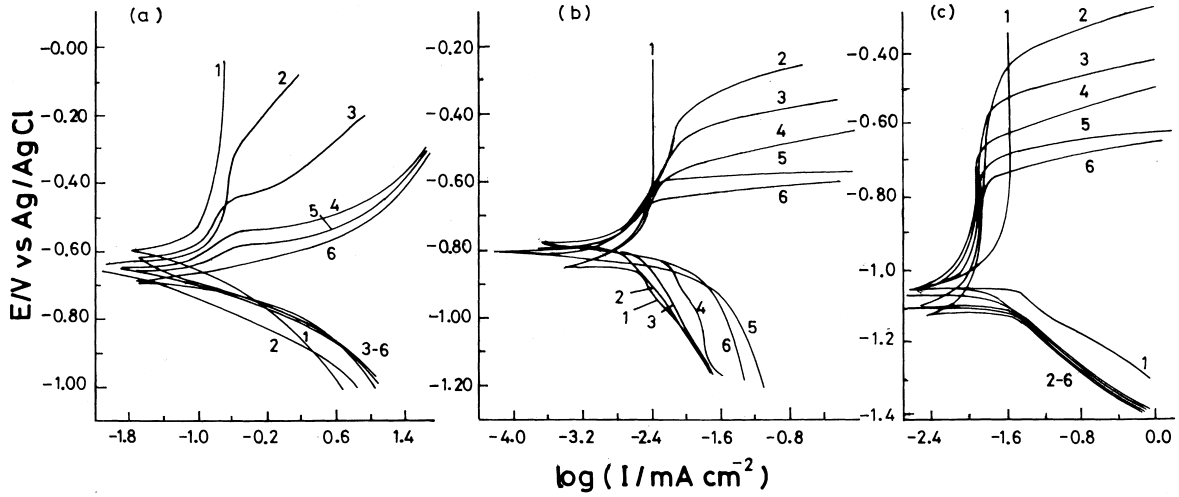

Fig. 8. Effect of Cl^- concentration (M) on the polarization curves of alloy II, (a) pH 2 [(1) 0.00, (2) 0.001, (3) 0.005, (4) 0.01, (5) 0.025 and (6) 0.06] (b) pH 7 [(1) 0.00, (2) 0.01, (3) 0.025, (4) 0.10, (5) 0.25 and (6) 0.50] and (c) pH 10 [(1) 0.00, (2) 0.05, (3) 0.10, (4) 0.25, (5) 0.50 and (6) 1.00].

the oxide film, since anions such as Cl^- are capable of displacing OH^- from the vicinity of the electrode surface [35]. Thus i_{corr} first increases with Cl^- concentration. At higher Cl^- concentrations, removal of more OH^- from the surface leads to increased adsorption of both SO_4^{2-} and Cl^- through the synergistic effect and slows down the attack, the net effect is a decrease in corrosion. The trend in increase or decrease of i_{corr} with NaCl concentration was found to be determined by the ratio of SO_4^{2-} to Cl^- during corrosion of Al–Zn–Mg alloy [36].

At pH 10.0, i_{corr} values increase with Cl^- concentration, although these values are lower than the i_{corr} value recorded in absence of Cl^- ions. This is due to the observed decrease in both cathodic current and anodic current in the active region. Displacement of OH^- by Cl^- [35] at this pH reduces the corrosion rate due to reduction in alkalinity at the electrode surface, and as Cl^- concentration increases the attack also increases leading to higher i_{corr} values.

Comparison of i_{corr} values at one and the same Cl^- concentration revealed that the highest value is at pH 2.0 and the lowest at pH 7.0. Taking into account the adherent film that forms in neutral environments on aluminium surfaces, the results are in accord with the enhanced solubility in both acidic and alkaline (> pH 9.0) media [37].

The passivity regions observed in Figure 8 are pH dependent. As mentioned before, this region decreases with increases in Cl^- concentration at a definite pH value. At the same Cl^- concentration, this region is largest at pH 10.0 and smallest at pH 2.0. This is attributed to the type of charge on the surface at different pH values. At pH 2.0, and to less extent at pH 7.0, the surface is probably positively charged [14], while it is negatively charged at pH 10.0. Chloride ions will be directly attached to the positively charged surface, which leads to the observed small passivity region at pH 2.0, and the increase in i_{corr} with Cl^- concentration. On the other hand, at pH 10.0, protonated water will adsorb on the negatively charged surface, giving rise to passive conditions, when conditions favour formation of the hydroxide precipitate. The chloride ions which are bonded chemically to the surface [18] lead to the formation of different mixed oxo-, hydroxo- and chlorocomplexes which finally produce $(AlCl_6)^{3-}$, leading to breakdown of passivity.

Due to the decrease in passivity with increase in Cl^- concentration, E_{pit} shifts to more negative values, corresponding to decrease in protection of the film formed on the electrode surface. This decrease in E_{pit} values is attributed to the reduction of the hindrance of oxide/salt transformation [16]. In neutral and acid media transitional chloride complexes are formed [10], according to Equation 1, while oxo-, hydroxo- and chlorocomplexes are formed in alkaline media [18]. Finally, $(AlCl_6)^{3-}$ is produced and competes with formation of $Al(OH)_3$. At E_{pit} the formation of soluble species is the cause of breakdown of the passive layer [10, 18, 29].

The relation between E_{pit} and Cl^- concentration, shown in Figure 9, may be put in the form:

$$E_{pit} = E^{\circ}_{pit} - \frac{2.3RT}{nF}\log[Cl^-] \qquad (5)$$

where E°_{pit} is the value of E_{pit} at unit concentration of Cl^-, n is the reaction order or the number of Cl^- ions in the complex formed during the rate determining step in the pitting process. A similar relation between E_{pit} and Cl^- concentration was reported [29].

The slopes of the relations in Figure 9 are equal at high and low pH values, while the value at neutral pH is lower. Similar results were reported for aluminium in chloride media [38]. Thus, destruction of the anodic film is facilitated at low and high pH values. Values of the intercept E°_{pit} at pH 2.0, 10.0 and 7.0 are −0.990, −0.760 and −0.715 V, respectively. The most negative value is obtained at pH 2.0, indicating that pitting initiates more readily at this pH value.

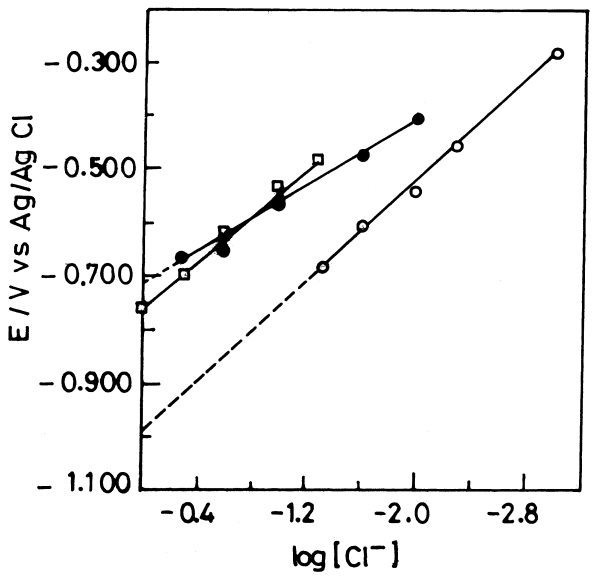

Fig. 9. Relation between E_{pit} and Cl^- concentration at pH (O) 2.0, (△) 7.0 and (●) 10.0.

The mechanism of pitting corrosion by Cl^- was proposed [39]. Cl^- increase the relative rate of film breakdown reaction. Increase in Cl^- concentration and potential lead to an increase in the rate of film breakdown. Onset of pitting is attributed to the domination of this reaction over the film forming reaction at the base of the flaw in the film. This explains the shift of E_{pit} towards the active direction. Above E_{pit}, corrosion occurs within the pits by formation of a salt film [13]. A pit-like morphology was reported to develop under the compact layer, which grew to larger cavities and became sites of localized attack [40].

4. Conclusions

(i) Al–Si alloys corrode in HCl solutions more than pure aluminium in the order II > I > III > Al, due to formation of localized galvanic couples in the alloys. While the attack is of the general type in case of aluminium metal, different stages of pitting are observed in case of the alloys, being more severe in case of alloy II. The high corrosion rates of alloy II is attributed to its high content of the eutectic as compared to the other two alloys.

(ii) Loss of protection by the native oxide film on extended immersion of the alloys in HCl is reflected in departure from capacitive to resistive behaviour of the oxide covered electrode, reflected by decrease of θ with time.

(iii) Shift of E_{corr} to positive values with HCl concentration is mainly due to a decrease in the pH of the solution.

(iv) At neutral pH, the trend in increase or decrease of corrosion rate as reflected in i_{corr} values, depends on the Cl^- concentration; while at pH 10.0, addition of Cl^- ions initially decreases the corrosion rate.

(v) Film breakdown and pitting at pH 2.0 is facilitated by the positive charge on the oxide surface at low pH values which leads to attraction of Cl^- ions and attack of the oxide film.

Acknowledgement

A.A. Mazhar thanks the Alexandar von Humboldt Foundation for providing facilities for EIS studies, and Prof. H. Abd El-Rahman for permission to use these facilities.

References

1. F. Ovari, L. Tomcsanyi and T. Turmezey, *Electrochim. Acta* **33**(3) (1988) 323.
2. D.M. Drazic, S.K. Zecevic, R.T. Atanasoki and A.R. Despic, *Electrochim. Acta* **28** (1983) 751.
3. J.L. Murray and A.J. McAlister, *Bull. Alloy Phase Diag.* **5**(1) (1984) 74.
4. H. Bohni and H.H. Uhlig, *J. Electrochem. Soc.* **116** (1969) 906.
5. F. Holzer, S. Müller, J. Desilvestro and O. Haas, *J. Appl. Electrochem.* **23** (1993) 125.
6. G. Buri, W. Luedi and O. Haas, *J. Electrochem. Soc.* **136** (1989) 2167.
7. M. Elboujdaini, E. Ghali, R.G. Barradas and M. Girgis, *Corr. Sci.* **30**(8, 9) (1990) 855.
8. T. Hagyard and W.E. Earl, *J. Electroanal. Chem.* **182** (1985) 179.
9. E. Deltombe, C. Vanleugenhaghe and M. Pourbaix, '*Atlas of Electrochemical Equilibria in Aqueous Solutions*', 2nd edn (NASA, Houston, TX, 1974), p. 168.
10. R. Ambat and E.S. Dwarakadasa, *Br. Corr. J.* **28**(2) (1993) 142.
11. B.R. Baker and J.D. Balser, *Aluminium* **52** (1976) 197.
12. F.D. Bogar and R.T. Foley, *J. Electrochem. Soc.* **119** (1972) 462.
13. W.M. Moore, C. Chen and G.A. Shirn, *Corrosion* **40**(12) (1984) 644.
14. G.A. Parks, *Chem. Rev.* **65** (1965) 177.
15. C.M.A. Brett, *J. Appl. Electrochem.* **20** (1990) 1000.
16. F. Hunkeler, G.S. Frankel and H. Bohni, *Corrosion* **43**(3) (1987) 189.
17. K.J. Vetter and H.H. Strehblow, '*Localized Corrosion*' (NACE, Housten, TX, 1974), pp. 240–51.
18. L. Tomcsanyi, K. Varga, I. Bartik, G. Horanyi and E. Maleczki, *Electrochim. Acta* **34**(6) (1989) 855.
19. T.U. Chavanin, *Corrosion* **47**(6) (1991) 472.
20. M. Stern and A.L. Geary, *J. Electrochem. Soc.* **104** (1957) 56.
21. A.M. Beccaria and G. Poggi, *Corrosion* **42**(8) (1986) 470.
22. M. Metikos-Hukovic, R. Babic, Z. Grubac and S. Brinic, *J. Appl. Electrochem.* **24** (1994) 772.
23. A. Conde and J. de Damborenea, *Electrochim. Acta* **43**(8) (1998) 849.
24. J. Titz, G.H. Wagner, H. Spähn, M. Ebert, K. Jüttner and W.J. Lorenz, *Corrosion* **46**(3) (1990) 221.
25. J.B. Bessone, D.R. Salinas, C.E. Mayer, M. Ebert and W.J. Lorenz, *Electrochim. Acta* **37** (1992) 2283.
26. D.D. Macdonald, *J. Electrochem. Soc.* **125** (1978) 2063.
27. K.S.N. Murthy and E.S. Dwarakadasa, *Br. Corros. J.* **30**(2) (1995) 111.
28. A.J. Griffin, Jr., F.R. Brotzen and C.F. Dunn, *J. Electrochem. Soc.* **139** (1992) 699.
29. R. Ambat and E.S. Dwarakadasa, *J. Appl. Electrochem.* **24** (1994) 911.
30. M. Tsutsui and T. Yamada, *J. Jpn Inst. Met.* **56**(3) (1992) 271.

31. C.B. Breslin, L.P. Friery and W.M. Corroll, *Corros. Sci.* **36**(1) (1994) 85.
32. W.M. Chan, F.T. Cheng, L.K. Leung, A.J. Horylev and T.M. Yu, *Corros. Rev.* **16**(1, 2) (1998) 43.
33. C.M.A. Brett, I.A.R. Gomes and J.P.S. Martins, *Corros. Sci.* **36**(6) (1994) 915.
34. A.M. McKissick, A.A. Adams and R.T. Foley, *J. Electrochem. Soc.* **117** (1970) 1459.
35. M. Reboul and P. Meyer, Proc. 4th International Aluminium – Lithium Conference, *J. Phys.* (*France*) **48** (1987), (suppl. C3) 881.
36. A.K. Bhattamishra and M.K. Banerjee, *Z. Metallkd.* **84**(10) (1993) 734.
37. N.G. Smart, R.C. Bhardwaj and J. O'M. Bockris, *Corrosion* **48** (1992) 764.
38. N. Lampeas and P.G. Koutsoukos, *Corros. Sci.* **36**(6) (1994) 1011.
39. R. Roth and H. Kaseche, Proceedings of 5th International Aluminium–Lithium Conference, Williamsburg VA, Vol. III (1989), p. 1207.
40. M.R. Tabrizi, S.B. Lyon, G.E. Thompson and J.M. Ferguson, *Corros. Sci.* **32**(7) (1991) 733.